Profiles of intraocular higher-order aberrations in healthy phakic eyes: prospective cross-sectional study

Jiaqing Zhang[#], Guangming Jin[#], Ling Jin[#], Xiaoting Ruan[#], Xiaoxun Gu, Wei Wang, Xiaoyun Chen, Lanhua Wang, Ye Dai, Zhenzhen Liu, Lixia Luo, Yizhi Liu

State Key Laboratory of Ophthalmology, Zhongshan Ophthalmic Center, Sun Yat-sen University, Guangzhou, China

Contributions: (I) Conception and design: Z Liu, L Luo; (II) Administrative support: Z Liu, L Luo; (III) Provision of study materials or patients: Z Liu, L Luo; (IV) Collection and assembly of data: J Zhang, G Jin, L Jin, X Ruan, X Gu, W Wang, X Chen, Y Dai, L Wang; (V) Data analysis and interpretation: J Zhang , G Jin, L Jin; (VI) Manuscript writing: All authors; (VII) Final approval of manuscript: All authors.

[#]These authors contributed equally to this work as co-first authors.

Correspondence to: Prof. Lixia Luo, MD, PhD; Dr. Zhenzhen Liu, MD, PhD. State Key Laboratory of Ophthalmology, Zhongshan Ophthalmic Centre, Sun Yat-sen University, Guangzhou, China. Email: luolixia@mail.sysu.edu.cn; liuzhenzhen@gzzoc.com.

Background: Ocular wavefront aberration is a crucial optical factor affecting retinal imaging. Internal aberrations contributed to compensation mechanism of ocular aberration. However, previous studies mainly focused on total and corneal higher order aberrations, and little is known about the profile of internal HOA (IHOA) in healthy subjects.

Methods: Participants with healthy crystalline lenses were prospective enrolled. The root mean square (RMS) of IHOAs for a pupil diameter of 4 mm were measured with an iTrace aberrometer. Lenticular parameters were measured with a swept source anterior segment optical coherence tomography (AS-OCT). Regression analyses were used to determine factors associated with logarithmic IHOAs.

Results: Sixty-six Chinese participants (132 eyes) ranging from 5 to 59 years were analyzed. Logarithmic IHOA was positively associated with axial length (AL) (coefficient =0.101, P=0.016), and negatively associated with ocular refraction (coefficient =–0.032, P=0.023). Logarithmic internal coma increased by 0.161/mm (P=0.016) as AL became longer and decreased by 0.081/diopter (P<0.001) as ocular refraction became hyperopic. Lens tilt (coefficient =–0.121, P=0.037), decentration (coefficient= 3.027, P=0.003), and radius of anterior lens surface curvature (RAL) (coefficient= 0.096, P=0.026) were associated with logarithmic internal trefoil. lens tilt was also associated with logarithmic internal spherical aberration (coefficient =–0.195, P=0.018) and second astigmatism (coefficient =–0.132, P=0.030). Binocularly, the extent of coma, trefoil was different, while that of spherical aberration, secondary astigmatism was consistent. The vectors of the same type of IHOAs were nearly paralleled.

Conclusions: IHOAs are mainly affected by ocular refraction, RAL, lens tilt and decentration. Intraocular differences and directions of higher-order aberrations follow certain rules, and their effects on visual function warrant further study.

Keywords: Intraocular aberration; crystalline lens; radius of anterior lens surface curvature; tilt; decentration

Introduction

Ocular wavefront aberration is one of the crucial optical factors affecting retinal imaging (1,2). It refers to the positional deviation between the ideal and the actual wavefront shape when comparing the imaging from the optical elements of actual eye to that from the standard optical components of model eye (3).

The technological advancements in wavefront

Page 2 of 9

Zhang et al. Binocular intraocular higher-order aberrations

aberrometry have allowed us for a thorough understanding of lower order aberrations. Nevertheless, most of the previous studies on higher order aberrations (HOA) focused on total and corneal HOA and little is known about the internal HOA(IHOA) (4-6). It has been reported that the aberrations of the anterior cornea and the internal lens are in a balanced, mutually compensated state, indicating that IHOA contributed to compensation mechanism of ocular aberration (7,8). Some researchers reported that the wavefront aberration of older eyes change with the severity and morphology of lens opacity (9-11). However, the baseline profile of IHOAs remains to be explored, and the characteristics of IHOAs in healthy population with transparent lenses have not been systematically investigated. What is more, the total and corneal ocular optical aberrations in the human visual system have been studied in reference to ocular symmetry, whereas the bilateral distribution of IHOAs in healthy people remains unclear (12-16).

We conducted this study to analyze the distribution, the major determinants, and binocular relationship of IHOAs in healthy lenses. We present the following article in accordance with the STROBE reporting checklist (available at http://dx.doi.org/10.21037/atm-20-1023).

Methods

Subjects and setting

This prospective cross-sectional study was conducted at the Zhongshan Ophthalmic Center, Sun Yat-sen University, Guangzhou, China. Participants were consecutively recruited from the outpatient department during August 2019 to September 2019. Exclusion criteria were presence of lens opacity, ocular diseases affecting anterior structures such as lens subluxation, glaucoma and ocular trauma, prior ocular pathology or surgery, an intraocular pressure (IOP) higher than 22 mmHg, and any category of amblyopia.

All the procedures in this study were conducted in accordance with the Declaration of Helsinki (as revised in 2013) and arranged strictly with the approval of the institutional review board of Zhongshan Ophthalmic Centre of Sun Yat-sen University (IRB-ZOC-SYSU, 2019KYPJ033). All participants have written informed consent prior to the measurements.

Ocular examination

The early treatment of diabetic retinopathy study (ETDRS)

LogMAR E chart (Precision Vision, Villa Park, Illinois, USA) was used to conduct a visual acuity test including naked visual acuity (NVA) and BCVA. The cycloplegic ocular refraction was determined by Nidek (Gamagori, Japan) ARK-700 autorefractometer. The compound tropicamide eyedrops (Sinqi Pharmaceutical, ShenYang, China), which were composed of 5mg tropicamide and 5mg norepinephrine hydrochloride in 1ml, were used before refraction measurement. The slit lamp bio-microscope (BQ-900, Haag-Streit, Switzerland) and the ophthalmoscope (YZ11D, Suzhou, China) were used to evaluate the anterior and posterior segments. The noncontact tonometer (CT-1 Computerized Tonometer, Topcon Ltd, Topcon) was used for IOP measurements and the average value for three consecutive measurements was recorded. The IOL master 700 (Carl Zeiss Meditec AG, Jena, Germany) was used to obtain ocular axial length (AL).

Measurement of ocular aberrations

Ocular aberrations were measured with iTrace (Tracey Technologies, Houston, TX, USA) aberrometry before administration of cycloplegic agent and refraction examination. The instrument uses laser ray-tracing technology to project an infrared beam into the eye and analyze the retinal spot pattern to determine wavefront aberrations. The mydriatic agent was not used throughout the examination and the luminance of the examination room was kept constant below 0.1 lux. Internal optic aberration was measured at pupil diameters of 4.0 mm. The average value of three consecutive measurements was used. Internal total RMS high order aberration (hereafter refers to as IHOA), coma aberration [Z(3,−1), Z(3,1)], trefoil aberration [Z(3,−3), Z(3,3)], spherical aberration [Z(4,0)], and secondary astigmatism (SA) [Z(4,−2), Z(4,2)] were measured.

SS-OCT imaging

Anterior segment imaging was performed with a commercial SS-OCT (CASIA-2; Tomey Corporation, Nagoya, Japan), which uses a swept source laser with a wavelength of 1,310-nm at a velocity of 30,000 A-scan/second. The mydriatic agent was not used for the measurement. The subjects were asked to sit and fixate on the external lights during the examination, so scanning was focused on the central cornea to obtain qualified cross-sectional images of the anterior segment. Images with severe artefacts were excluded including motion artefacts, data loss

due to blinking. Anterior segment and lens biometric parameters including anterior chamber depth (ACD), lens thickness (LT), lens diameter (LD), radius of anterior lens surface curvature (RAL), radius of posterior lens surface curvature (RPL), lens tilt (TILT) and decentration (DEC) were automatically quantified by built-in software. An independent author reviewed all the SS-OCT images.

Statistical analysis

Descriptive statistics for continuous variables were presented as mean ± standard deviation. The Kolmogorov-Smirnov test was used to determine if the data were normally distributed. The natural logarithmic transformation (base e) was used in linear regression analyses to approximate HOA data to a normal distribution. Linear regression analyses were applied to identify the determinants of HOAs using the data of the right eyes. All variables with P<0.20 in the single factor analysis were included in the stepwise multiple linear regression analysis. Similarly, variables which were significant at a level of <0.20 in the single-factor analysis were included in the multiple mixed-effect linear model (17). The paired t-test and Bland-Altman plot were used for comparing the differences of each type of IHOAs between right eye and left eye. The centroids of directional IHOAs were calculated as following: firstly, the corresponding x and y coordinates were calculated according to the length (Z) and the angle (α) of the vector. The following equator was used: x = cosα*Z and y = sinα*Z. Secondly, the aggregated lengths of the vectors for the same type of aberration was calculated using the following equator: $Z(aggregated) = \sqrt{meanX^2 + meanY^2}$. The angle of the aggregated vector of the IHOA was using the following equator: $α(total) = atan(\frac{meanY}{meanX})$. All statistical analyses were performed using Stata MP 15.0 (StataCorp LP, College Station, Texas, USA). A value of P<0.05 was considered to have statistical significance. Scatter plots and Bland-Altman plots were plotted with GraphPad Prism 6 (GraphPad Software, San Diego California, USA).

Results

Subject characteristics

Sixty-six subjects, [34 males (51.5%), 32 females (48.5%)], were included in the current analyses. The average age of the subjects was 17.22±11.92 years. One right eye and eight left eyes were excluded because of pupil size less than 4.0 mm. For the remainders, the mean spherical equivalent refraction of right eyes and left eyes were –2.12±1.86 diopters (D) and –2.22±2.16 D, respectively.

Association between age and IHOAs

The results of the linear regression analyses of age-related changes in IHOAs using data from the right eyes are summarized in Table S1. Logarithmic total IHOAs did not increase or decrease in the internal components with increasing age (all P>0.05). Gender-adjusted linear regression modeling validated no significance increase or decrease in logarithmic HOAs of the internal components for every year of age (all P>0.05). IHOA had no significant associations with age in our data set.

Ocular and lenticular factors associated with IHOAs

All Factors were plotted with each type of IHOAs, and those either with a P value smaller than 0.200 or of clinical relevance were shown in Figure 1. The association between ocular and lenticular factors with logarithmic HOAs using data from the right eyes are summarized in Table 1. Stepwise regression analysis showed that logarithmic IHOAs were associated with ocular and lenticular indexes. Axial length (AL) was positively associated with logarithmic IHOA (coefficient =0.101, P=0.016), whereas the SE was negatively associated with logarithmic IHOA (coefficient =–0.032, P=0.023). Internal logarithmic coma RMS decreased by 0.081/diopter (P<0.001) as the refractions became more hyperopic. Logarithmic internal trefoil RMS increased by 3.027/degree (P=0.003) as the extent of lens decentration increased. Logarithmic trefoil was positively associated with the RAL (coefficient =0.096, P=0.026), negatively with the extent of lens tilt (coefficient =–0.121, P=0.037). Internal spherical aberration and SA were both negatively correlated with lens tilt (coefficient =–0.195, P=0.018 and coefficient =–0.132, P=0.030).

Bilateral distribution of IHOAs

The results of the inter-ocular comparison using the absolute values of IHOAs are summarized in Table 2. Paired t-test showed that significant differences existed in IHOA (P=0.017), coma (P=0.017) and trefoil (P=0.045) between eyes. There was no significant difference in spherical aberration and SA between eyes (all P>0.05). Bland-Altman plots demonstrated that the 95% confidence interval of interocular differences were approximately (–0.3, 0.3) μm for total IHOAs, coma and trefoil, and (–0.1, 0.1) μm for spherical aberration and SA (Figure 2A,B,C,D,E). The
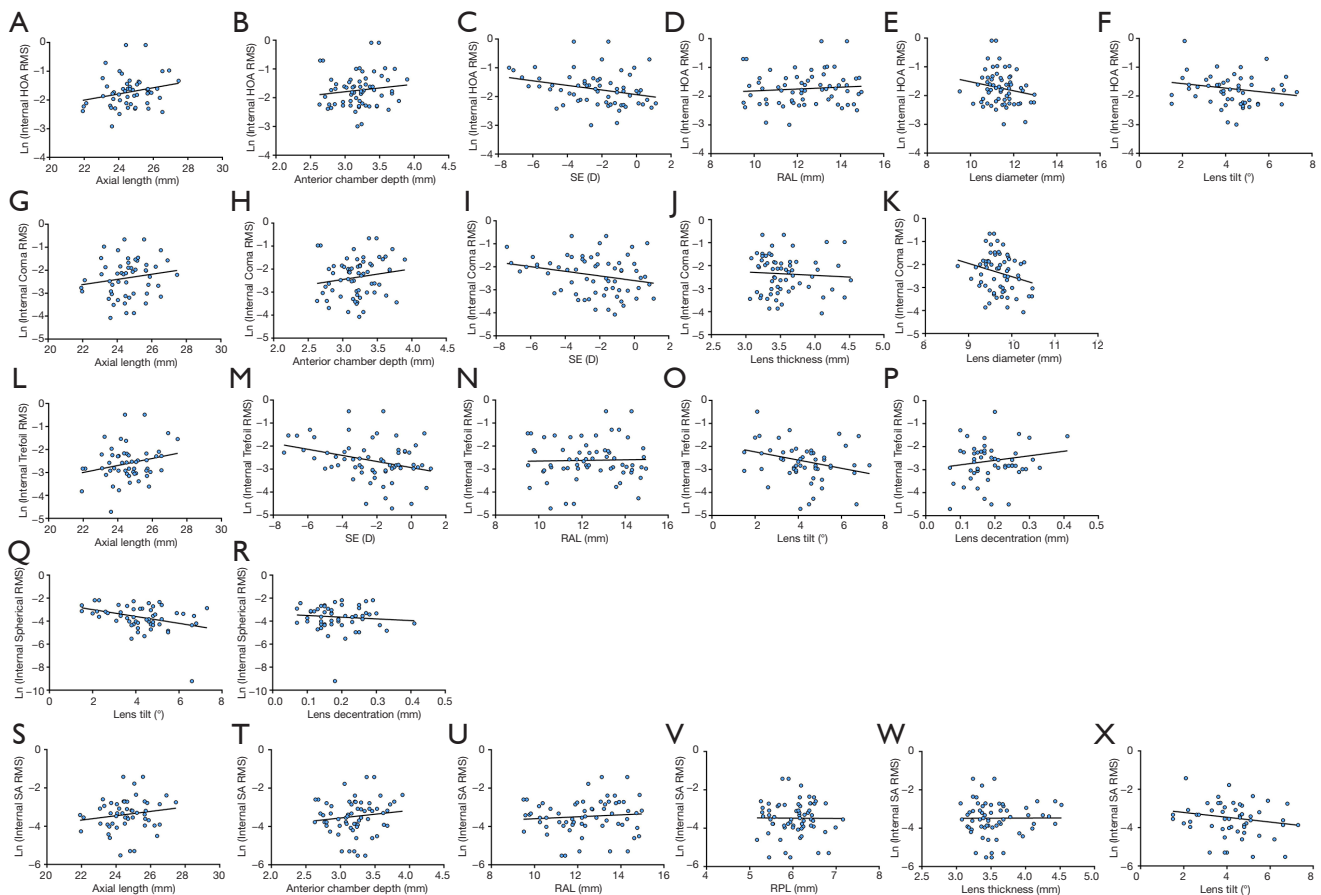
Figure 1 Scatter plots indicating the correlation of ocular and lenticular factors with IHOAs. Note: using data from right eyes. (A) Logarithmic internal higher order aberration (IHOA) RMS *vs.* axial length (P=0.092). (B) Logarithmic IHOA RMS *vs.* anterior chamber depth (ACD) (P=0.288). (C) Logarithmic IHOA RMS *vs.* spherical equivalent (SE) (P=0.019). (D) Logarithmic IHOA RMS *vs.* radius of anterior lens surface curvature (RAL) (P=0.479). (E) Logarithmic IHOA RMS *vs.* lens diameter (P=0.139). (F) Logarithmic IHOA RMS *vs.* lens tilt (P=0.130). (G) Logarithmic internal coma RMS *vs.* axial length (P=0.238). (H) Logarithmic internal coma RMS *vs.* ACD (P=0.194). (I) Logarithmic internal coma RMS *vs.* SE (P=0.040). (J) Logarithmic internal coma RMS *vs.* lens tilt (P=0.620). (K) Logarithmic internal coma RMS *vs.* lens diameter (P=0.058). (L) Logarithmic internal trefoil RMS *vs.* AL (P=0.085). (M) Logarithmic internal trefoil RMS *vs.* SE (P=0.009). (N) Logarithmic internal trefoil RMS *vs.* RAL (P=0.842). (O) Logarithmic internal trefoil RMS *vs.* lens tilt (P=0.020). (P) Logarithmic internal trefoil RMS *vs.* lens decentration (P=0.187). (Q) Logarithmic internal spherical RMS *vs.* lens tilt (P=0.002). (R) Logarithmic internal spherical RMS *vs.* lens decentration (P=0.435). (S) Logarithmic internal secondary astigmatism (SA) RMS *vs.* AL (P=0.250). (T) Logarithmic internal SA RMS *vs.* ACD (P=0.305). (U) Logarithmic internal SA RMS *vs.* RAL (P=0.471). (V) Logarithmic internal SA RMS *vs.* RPL (P=0.949). (W) Logarithmic internal SA RMS *vs.* lens thickness (P=0.972). (X) Logarithmic internal SA RMS *vs.* lens tilt (P=0.114). Ln: logarithmic, the natural logarithmic transformation (base e) was used in linear regression analyses to approximate HOA data to a normal distribution. RMS, root mean square; RAL, radius of anterior lens surface curvature; D, Diopter.

directions of the centroids of coma, trefoil, and SA were nearly paralleled between eyes respectively (*Figure 2F*).

Discussion

This prospective cross-sectional study measured the

IHOAs in non-cataract phakic eyes with an average age of seventeen years. The average IHOA value of all valid data is 0.212 µm for right eyes and 0.166 µm for left eyes in our study. Atchison *et al.* reported larger IHOAs (0.273 µm) than our study because they used a larger pupil zone of wavefront data (18). Namba *et al.* reported smaller IHOAs

Table 1 Associations of ocular and lenticular factors with logarithmic IHOAs

Aberration	Factors	Simple regression		Stepwise multi-factor	
		Coefficient (95% CI)	P	Coefficient (95% CI)	P
T-IHOA	AL	0.096 (0.017–0.175)	0.018*	0.101 (0.019–0.184)	0.016*
	ACD	0.222 (−0.092–0.536)	0.164		
	SE	−0.038 (−0.065−−0.010)	0.007*	−0.032 (−0.060−−0.005)	0.023*
	RAL	0.041 (−0.014–0.097)	0.144		
	DIA	−0.178 (−0.445–0.090)	0.191	−0.208 (−0.505−−0.089)	0.168
	TILT	−0.080 (−0.152−−0.007)	0.030*	−0.064 (−0.141−−0.013)	0.104
Coma	AL	0.142 (0.015–0.270)	0.029*	0.161 (0.031–0.293)	0.016*
	ACD	0.488 (0.011–0.964)	0.045*		
	SE	−0.084 (−0.125−−0.043)	<0.001*	−0.081 (−0.122−−0.040)	0.000*
	LT	−0.038 (−0.734–0.101)	0.136		
	DIA	−0.359 (−0.771–0.053)	0.087	−0.0458 (−0.936–0.019)	0.060
Trefoil	AL	0.142 (0.024–0.259)	0.019*		
	SE	−0.047 (−0.089−−0.004)	0.032*		
	RAL	0.071 (−0.015–0.156)	0.106	0.096 (0.012–0.181)	0.026*
	TILT	−0.167 (−0.276−−0.058)	0.003*	−0.121 (−0.234−−0.008)	0.037*
	DEC[#]	0.990 (−0.884–2.864)	0.298	3.027 (1.079–4.975)	0.003*
Spherical	TILT	−0.225 (−0.383−−0.067)	0.006*	−0.195 (−0.358−−0.034)	0.018*
	DEC	−2.839 (−5.498−−0.179)	0.037*	−2.070 (−4.755–0.614)	0.129
SA	AL	0.117 (−0.007–0.241)	0.063		
	ACD	0.525 (0.053–0.998)	0.030*	0.503 (−0.015–1.020)	0.057
	RAL	0.097 (0.013–0.181)	0.024*		
	RPL	0.261 (−0.053–0.576)	0.102		
	LT	−0.330 (−0.742–0.081)	0.114		
	TILT	−0.139 (−0.248−−0.029)	0.014*	−0.132 (−0.251−−0.012)	0.030*

Logarithmic aberration data from right eyes were used. The variables with a P value than 0.200 in the single-factor analysis are shown on the table. AL and SE entered the multi-factor model respectively. In the multi-factor model including AL or SE, the trend of other factors is consistent, and the coefficients are filled in according to the AL model. *, statistically significant (P<0.05); #, included in the Stepwise analysis because of clinical relevance. AL, axial length; ACD, anterior chamber depth; SE, spherical equivalent of ocular refraction; RAL, radius of the anterior lens surface curvature; RPL, radius of posterior lens surface curvatures; DIA, lens diameter; LT, lens thickness; TILT, the extent of lens tilt; DEC, the extent of lens decentration; CI, confidence intervals; T-IHOA, total internal higher order aberration; SA, Secondary astigmatism.

(0.087 μm) than our study, probably due to differences in the instruments and methods for calculating IHOAs (19). Our IHOA values are similar to the IHOA results reported by Philip *et al.* (0.19 μm), which may be related to the same race and similar average age of population (20).

Our current study revealed that IHOAs were mainly affected by the lenticular parameters and the refractive status of the eye. We firstly observed that the internal trefoil RMS were correlated with the radius of anterior lens surface curvature. Furthermore, the associations of the extent of lens tilt *vs.* IHOAs including trefoil, spherical aberration and SA were identified by both single and multi-

Page 6 of 9

Zhang et al. Binocular intraocular higher-order aberrations

Table 2 Interocular comparison of IHOA

Variable	OD		OS		P value
	Mean/centroid	SD (μm)	Mean/centroid	SD (μm)	
IHOA	0.212 μm	0.17	0.166 μm	0.06	0.017*
Coma	0.09 μm@86°	0.16	0.06 μm@88°	0.10	0.017*
Trefoil	0.06 μm@64°	0.15	0.04 μm@61°	0.08	0.045*
Spherical	−0.001 μm	0.05	−0.017 μm	0.05	0.066
SA	0.02 μm@68°	0.06	0.01 μm@3°	0.04	0.159

*, statistically significant. OD, right eye; OS, left eye; SD, standard deviation; IHOA, internal higher order aberration; SA, secondary astigmatism; μm, micrometer.
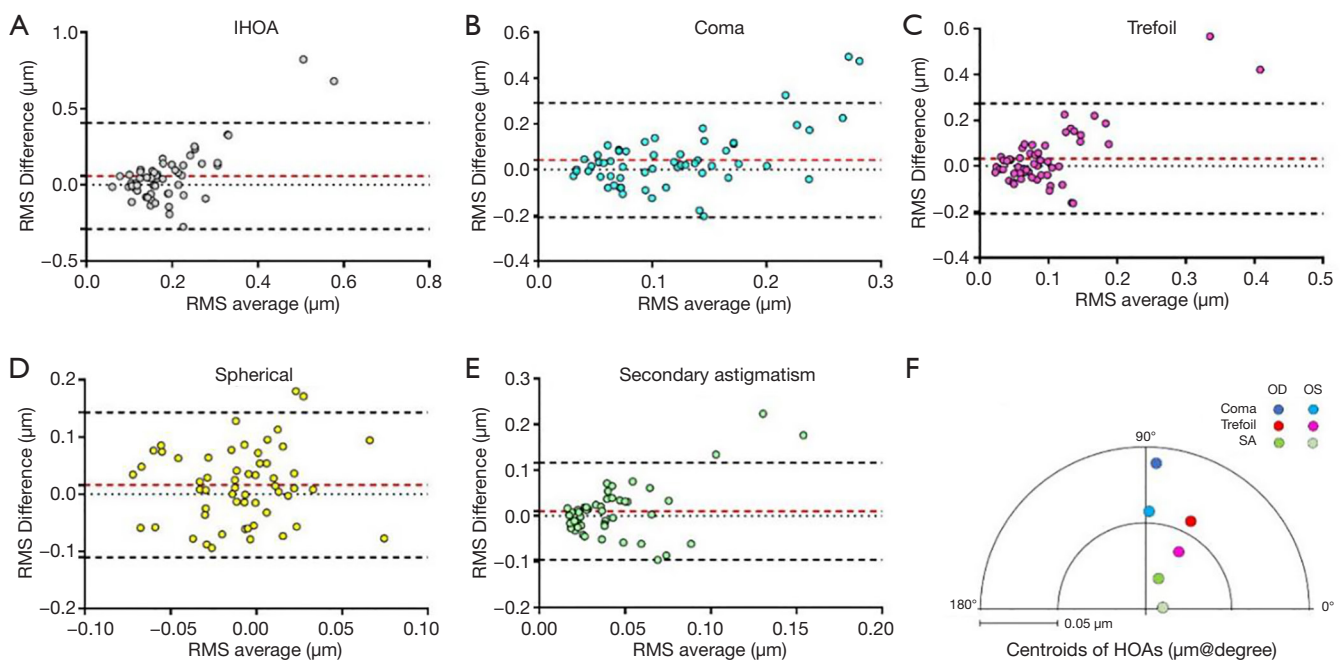
Figure 2 Bland-Altman plots indicating the agreement between internal wavefront aberrations of both eyes. (A) Total internal higher order aberration (IHOA): paired-T: P=0.017; (B) internal coma RMS: paired-T: P=0.017; (C) internal trefoil RMS: paired-T: P=0.045; (D) internal spherical RMS: paired-T: P=0.066; (E) internal secondary astigmatism (SA) RMS: paired-T: P=0.159. Reference lines correspond to the mean refractive errors (red) and 95% confidence intervals of the refractive errors (black). (F) Centroids of IHOAs in Both Eyes. Paired-T, paired samples *t*-test; RMS, root mean square; OD, right eye; OS, left eye; μm, micrometer.

factor analyses in our study, confirming geometrical features of crystalline lens as a major determinant of IHOAs. Berrio *et al.* suggested that geometrical variations in lens modified its aberrations and contributed to compensation mechanism of ocular aberration (21). Our results provide some preliminary clues of the underlying mechanisms.

Our data show that SE was negatively correlated with IHOA, internal coma, and trefoil. These findings indicate

that IHOAs decreased as the ocular refractions became more hyperopic. These results were consistent with previous study from other research groups (15,22). No similar relationship was observed by Philip *et al.* in IHOA and internal coma (20). Different instruments, pupil size, and study design influenced the direct comparison of our results. However, it has been reported that the emmetropic adult had the smallest aberrations compared with myopic

adults and children (23). Previous studies also showed that HOA decreased from childhood to early adulthood, and then increased with age (23,24). The early decline of HOA may be related to the process of emmetropization (22,23,25). Most of subjects included in our study were myopic. Whether there is a turning point for the trend of IHOAs, that the IHOAs are minimal at emmetropic status and become larger when the refractions are more hyperopic or myopic, is worth exploring. The associations of AL *vs.* internal total HOA were confirmed by both single and multi-factor analyses in our study , which is consistent with previous study. Lau *et al.* also found a relationship between axial length and ocular HOAs including trefoil and spherical aberration (26).

The relationship between age and HOAs remains controversial, and researches on the association between age and IHOA are limited. Our study found that IHOA were not significantly associated with aging in subjects with healthy lenses, which was consistent with Berrio *et al.* and Atchison *et al.* (21,27). IHOA value of cataract-free population were all significantly lower compared with the cataract eyes reported previously, suggesting that the increase of IHOA with aging is probably due to lens opacity (10,11).

Our results show that the binocular numerical differences of the internal coma and trefoil were significant, whereas the extent of spherical aberration and SA are bilateral consistent. The aggregated centroids of each type of IHOAs shows that the vector direction of the same type of IHOA is bilateral nearly parallel. To the best of our knowledge, this is the first study on the binocular profile of IHOAs. The combinations of different values and directions of the same type of aberration between two eyes may have complex effects on the binocular visual function. Previous studies have shown that the binocular symmetry of the total and corneal wavefront aberrations existed (14,15,28). As mentioned above, the aberrations of different optic components of the eye have a compensatory effect. For example, an increase in higher order aberrations with aging leads to a loss of balance, which causes a decrease in visual quality (29,30). At the same time, the accompanying change of the pupil and accommodating can compensate for the deterioration caused by the above process (8,31,32). How the binocular cornea HOA and IHOAs interact and compensate for each other and affect visual quality need to be addressed in further research.

The results of this study should be assessed within

the context of its limitations. First, the cross-sectional study design, rather than a longitudinal study, restricts us to evaluate the association between age and IHOA individually over time. Second, the sample size is small to obtain a more accurate linear assumption for analysis of various determinants of IHOAs. The subjects included in this study were mostly young and displayed large age-variations. The characteristics of the subjects may influence the investigation on the age-related changes. Thirdly, we calculated the centroids of IHOAs to analyze and compare their directionality. Notably, some anatomical parameters, such as the tilt and decentration of the crystalline lens, are also directional. Further researches on the influences caused by the directionality of these factors are warranted.

Conclusions

Previous studies have suggested that internal aberrations are mainly originated from the lens, but the relationship between IHOA and various biometric parameters of the lens remains to be elucidated. We have comprehensively analyzed the relationship between IHOAs and ocular refraction, axial length, and lens biometric parameters in non-cataract phakic population. Our findings suggest that IHOA are related to the refractive state of the eye and the geometrical features of the lens. The bilateral distribution of IHOAs was also explored. The vector direction of the same type IHOA is bilaterally paralleled. The binocular relative distribution of IHOAs and the effect on the visual function are worthy of further study.

Acknowledgments

Footnote

Reporting Checklist: The authors have completed the STROBE reporting checklist. Available at http://dx.doi.org/10.21037/atm-20-1023

Data Sharing Statement: Available at http://dx.doi.org/10.21037/atm-20-1023

Peer Review File: Available at http://dx.doi.org/10.21037/

atm-20-1023

Conflicts of Interest: All authors have completed the ICMJE uniform disclosure form (available at http://dx.doi.org/10.21037/atm-20-1023). The authors have no conflicts of interest to declare.

Ethical Statement: The authors are accountable for all aspects of the work in ensuring that questions related to the accuracy or integrity of any part of the work are appropriately investigated and resolved. All the procedures in this study were conducted in accordance with the Declaration of Helsinki (as revised in 2013) and arranged strictly with the approval of the institutional review board of Zhongshan Ophthalmic Centre of Sun Yat-sen University (IRB-ZOC-SYSU). Written informed consents have been obtained from all participants.

Open Access Statement: This is an Open Access article distributed in accordance with the Creative Commons Attribution-NonCommercial-NoDerivs 4.0 International License (CC BY-NC-ND 4.0), which permits the non-commercial replication and distribution of the article with the strict proviso that no changes or edits are made and the original work is properly cited (including links to both the formal publication through the relevant DOI and the license). See: https://creativecommons.org/licenses/by-nc-nd/4.0/.

References

1. Oshika T, Okamoto C, Samejima T, et al. Contrast sensitivity function and ocular higher-order wavefront aberrations in normal human eyes. Ophthalmology 2006;113:1807-12.
2. Lombardo M, Lombardo G. Wave aberration of human eyes and new descriptors of image optical quality and visual performance. J Cataract Refract Surg 2010;36:313-31.
3. Mello GR, Rocha KM, Santhiago MR, et al. Applications of wavefront technology. J Cataract Refract Surg 2012;38:1671-83.
4. Dickman MM, Cheng YY, Berendschot TT, et al. Effects of graft thickness and asymmetry on visual gain and aberrations after descemet stripping automated endothelial keratoplasty. JAMA Ophthalmol 2013;131:737-44.
5. Kemraz D, Cheng XY, Shao X, et al. Age-Related Changes in Corneal Spherical Aberration. J Refract Surg 2018;34:760-7.
6. Plainis S PI. Ocular monochromatic aberration statistics in a large emmetropic population. J Mod Opt 2008;4-5:759-72.
7. Artal P, Guirao A, Berrio E, et al. Compensation of corneal aberrations by the internal optics in the human eye. J Vis 2001;1:1-8.
8. Tabernero J, Benito A, Alcon E, et al. Mechanism of compensation of aberrations in the human eye. J Opt Soc Am A Opt Image Sci Vis 2007;24:3274-83.
9. Lee JH, Choo HG, Kim SW. Spherical aberration reduction in nuclear cataracts. Graefes Arch Clin Exp Ophthalmol 2016;254:1127-33.
10. Zhu X, Ye H, He W, et al. Objective functional visual outcomes of cataract surgery in patients with good preoperative visual acuity. Eye (Lond) 2017;31:452-9.
11. Faria-Correia F, Lopes B, Monteiro T, et al. Scheimpflug lens densitometry and ocular wavefront aberrations in patients with mild nuclear cataract. J Cataract Refract Surg 2016;42:405-11.
12. Fam HB, Lim KL. Effect of higher-order wavefront aberrations on binocular summation. J Refract Surg 2004;20:S570-5.
13. Jimenez JR, Castro JJ, Jimenez R, et al. Interocular differences in higher-order aberrations on binocular visual performance. Optom Vis Sci 2008;85:174-9.
14. Cavas-Martínez F, Fernández-Pacheco D, Mira J, et al. Assessment of Pattern and Shape Symmetry of Bilateral Normal Corneas by Scheimpflug Technology. Symmetry 2018;10:453.
15. Hartwig A, Atchison DA. Analysis of higher-order aberrations in a large clinical population. Invest Ophthalmol Vis Sci 2012;53:7862-70.
16. Lombardo M, Lombardo G, Serrao S. Interocular high-order corneal wavefront aberration symmetry. J Opt Soc Am A Opt Image Sci Vis 2006;23:777-87.
17. Heinze G, Dunkler D. Five myths about variable selection. Transpl Int 2017;30:6-10.
18. Atchison DA, Suheimat M, Mathur A, et al. Anterior Corneal, Posterior Corneal, and Lenticular Contributions to Ocular Aberrations. Invest Ophthalmol Vis Sci 2016;57:5263-70.
19. Namba H, Kawasaki R, Narumi M, et al. Ocular higher-order wavefront aberrations in the Japanese adult population: the Yamagata Study (Funagata). Invest Ophthalmol Vis Sci 2014;56:90-7.
20. Philip K, Martinez A, Ho A, et al. Total ocular, anterior corneal and lenticular higher order aberrations in hyperopic, myopic and emmetropic eyes. Vision Res

2012;52:31-7.

21. Berrio E, Tabernero J, Artal P. Optical aberrations and alignment of the eye with age. J Vis 2010;10:34.

22. Yotsukura E, Torii H, Inokuchi M, et al. Current Prevalence of Myopia and Association of Myopia With Environmental Factors Among Schoolchildren in Japan. JAMA Ophthalmol 2019;137:1233-9.

23. He JC, Sun P, Held R, et al. Wavefront aberrations in eyes of emmetropic and moderately myopic school children and young adults. Vision Res 2002;42:1063-70.

24. Brunette I, Bueno JM, Parent M, et al. Monochromatic aberrations as a function of age, from childhood to advanced age. Invest Ophthalmol Vis Sci 2003;44:5438-46.

25. Kasahara K, Maeda N, Fujikado T, et al. Characteristics of higher-order aberrations and anterior segment tomography in patients with pathologic myopia. Int Ophthalmol 2017;37:1279-88.

26. Lau JK, Vincent SJ, Collins MJ, et al. Ocular higher-order aberrations and axial eye growth in young Hong Kong children. Sci Rep 2018;8:6726.

27. Atchison DA, Markwell EL. Aberrations of emmetropic subjects at different ages. Vision Res 2008;48:2224-31.

28. Arba Mosquera S, Verma S. Bilateral symmetry in vision and influence of ocular surgical procedures on binocular vision: A topical review. J Optom 2016;9:219-30.

29. Fujikado T, Kuroda T, Ninomiya S, et al. Age-related changes in ocular and corneal aberrations. Am J Ophthalmol 2004;138:143-6.

30. Namba H, Kawasaki R, Sugano A, et al. Age-Related Changes in Ocular Aberrations and the Yamagata Study (Funagata). Cornea 2017;36 Suppl 1:S34-40.

31. Lopez-Gil N, Fernandez-Sanchez V, Legras R, et al. Accommodation-related changes in monochromatic aberrations of the human eye as a function of age. Invest Ophthalmol Vis Sci 2008;49:1736-43.

32. He JC, Wang J. Measurement of wavefront aberrations and lens deformation in the accommodated eye with optical coherence tomography-equipped wavefront system. Opt Express 2014;22:9764-73.

Table S1 Linear regression analysis of the relationship between IHOAs and age

Variable	Linear regression analysis-logarithm				Gender-adjusted-logarithm		
	Starting value	Change per Y of age	95% CI	P value	Change per Y of age	95% CI	P value
Total IHOA	−1.784	−0.002	−0.010–0.006	0.625	−0.002	−0.010–0.006	0.654
Coma	−2.369	−0.005	−0.017–0.007	0.430	−0.005	−0.017–0.008	0.456
Trefoil	−2.640	−0.002	−0.015–0.010	0.690	−0.003	−0.015–0.010	0.658
Spherical	−3.573	−0.007	−0.024–0.011	0.440	−0.009	−0.027–0.009	0.320
SA	−3.438	−0.004	−0.016–0.008	0.505	−0.002	−0.015–0.010	0.690

IHOA, internal higher order aberration.